

Heterotrophic
prokaryote
distribution in the
NPSG

M. Girault et al.

This discussion paper is/has been under review for the journal Biogeosciences (BG).
Please refer to the corresponding final paper in BG if available.

Heterotrophic prokaryote distribution along a 2300 km transect in the North Pacific subtropical gyre during strong La Niña conditions: relationship between distribution and hydrological conditions

M. Girault¹, H. Arakawa², A. Barani³, H. J. Ceccaldi³, F. Hashihama², and G. Gregori³

¹Kanagawa Academy of Science and Technology, LISE 4C-3, 3-25-13 Tonomachi Kawasaki-ku, Kawasaki-shi, Kanagawa 210-0821, Japan

²Department of Ocean Sciences, Tokyo University of Marine Science and Technology, 5-7 Konan 4, Minato-ku, Tokyo 108-8477, Japan

³Aix-Marseille Université Mediterranean Institute of Oceanography MIO UM 110, Université de Toulon, CNRS/INSU, IRD, 13288, Marseille, CEDEX 09, France

Title Page

Abstract

Introduction

Conclusions

References

Tables

Figures

⏪

⏩

◀

▶

Back

Close

Full Screen / Esc

Printer-friendly Version

Interactive Discussion



Received: 8 October 2014 – Accepted: 11 October 2014 – Published: 14 November 2014

Correspondence to: M. Girault (girault.bmi@gmail.com)
and G. Gregori (gerald.gregori@univ-amu.fr)

Published by Copernicus Publications on behalf of the European Geosciences Union.

BGD

11, 15793–15826, 2014

**Heterotrophic
prokaryote
distribution in the
NPSG**

M. Girault et al.

Title Page

Abstract

Introduction

Conclusions

References

Tables

Figures



Back

Close

Full Screen / Esc

Printer-friendly Version

Interactive Discussion



abiotic variables (temperature, salinity, pressure, irradiance, nutrient concentrations). These possible limiting variables are shared with the autotrophic community and competition for resources inevitably occurs in order for each to survive in the same pelagic ecosystem. Competition between heterotrophic prokaryotes and phytoplankton for different forms of inorganic nitrogen and phosphorus has been clearly demonstrated both in laboratory experiments and in the open ocean (Currie and Kalff, 1984; Vadstein, 1998; Thingstad et al., 1998). Moreover, several studies have reported that dissolved organic compounds can be an alternative nutrient source for some nutrient-stressed phytoplankton (Duhamel et al., 2010; Girault et al., 2013a). The common utilization of the inorganic and/or organic matter, such as dissolved organic phosphorus, could lead to a tight coupling between the heterotrophic prokaryotes and photoautotrophs along an oligotrophic gradient. However, the relationship between heterotrophic prokaryote abundance and oligotrophic conditions is unclear, especially in terms of mesoscale structures such as eddies (Baltar et al., 2010; Lasternas et al., 2013). The differences within the same type of mesoscale circulation reported in the literature highlights that the relationship between heterotrophic prokaryotes and photoautotrophs can be dependent on the identification of the different microorganisms making up the community (Girault et al., 2013b).

In this study, using analytical flow cytometry combined with fluorescent dyes we were able to identify three different subgroups among the bulk of heterotrophic prokaryotes: a group characterized by a very high nucleic acid content (VHNA), another by a high nucleic acid content (HNA), and finally a group with a low nucleic acid content (LNA). Previous studies have reported that the more active microorganisms seem to have the higher nucleic acid contents (Gasol et al., 1999; Lebaron et al., 2001). Complementary results have suggested that heterotrophic prokaryote activities are influenced by environmental parameters especially under oligotrophic conditions (Zubkov et al., 2001; Grégori et al., 2001, 2003a; Nishimura et al., 2005; Sherr et al., 2006; Bouvier et al., 2007). Using the basis of these previous reports, the oligotrophic conditions investigated in the western part of the NPSG during the Tokyo–Palau Cruise enabled

Heterotrophic prokaryote distribution in the NPSG

M. Girault et al.

Title Page

Abstract

Introduction

Conclusions

References

Tables

Figures



Back

Close

Full Screen / Esc

Printer-friendly Version

Interactive Discussion



estimated according to the $\Delta\sigma_\theta = 0.15 \text{ kg m}^{-3}$ (relative to $z = 10 \text{ m}$; Thomson and Fine, 2003). The irradiance was monitored at five stations (5, 7, 9, 11, 12) using a Profiling Reflectance radiometer (PRR 600 Biospherical Instrument[®]). The depth of the euphotic layer was estimated as the depth of 1 % of photosynthetically active radiation at noon.

2.2 Altimetry and large scale climatic conditions

The altimetry data (sea level anomaly) was produced by Ssalto/Duacs and distributed by Aviso, with support from CNES (<http://www.aviso.oceanobs.com/duacs/>). The sea level anomaly map centered on the 18 January 2011 was plotted using the Panoply software from NASA (<http://www.giss.nasa.gov/tools/panoply/>). This map was processed by compiling the data collected over a six weeks period before and after the chosen date (Fig. 1). The current sea maps provided by the bulletin of the Japanese coast guard were used to validate the satellite data and display the paths of both the cyclonic gyre and the Kuroshio Stream (http://www1.kaiho.mlit.go.jp/KANKYO/KAIYO/qboc/index_E.html).

2.3 Nutrient analyses

Nutrient samples were collected from Niskin bottles, immediately put into cleaned plastic tubes in the dark, plunged into liquid nitrogen and stored in the deep freeze (-60°C) until analyses. The highly sensitive colorimetric method incorporating the AutoAnalyzer II (SEAL Analytical) and Liquid Waveguide Capillarity Cells (World precision Instruments), was used to determine nutrient concentrations (nitrate + nitrite, soluble reactive phosphorus and silicic acid) according to the methods listed in Hashihama et al. (2009) and Hashihama and Kanda (2010). Seawater collected at the surface of the western part of NPSG, which had been preserved for > 1 year, was used as nitrate + nitrite blank water. The blank water was analyzed using the chemiluminescent method described in Garside (1982). The detection limits for nitrate + nitrite, soluble reactive phosphorus and silicic acid were 3, 3 and 11 nM, respectively.

Heterotrophic prokaryote distribution in the NPSG

M. Girault et al.

Title Page

Abstract

Introduction

Conclusions

References

Tables

Figures

◀

▶

◀

▶

Back

Close

Full Screen / Esc

Printer-friendly Version

Interactive Discussion



Because soluble reactive phosphorus consists mainly of orthophosphate and nitrite was not substantially detectable, soluble reactive phosphorus and nitrate + nitrite are hereafter referred to as phosphate and nitrate.

2.4 Chlorophyll *a* and flow cytometry analyses

5 The depth of the deep chlorophyll *a* maximum was determined from fluorescence profiles using the pre-calibrated in situ fluorometer. To measure chlorophyll *a* concentration, 250 cm³ of seawater was filtrated through Whatman[®] nucleopore filters (porosity ~ 0.2 μm) using a low vacuum pressure (< 100 mm of Hg). Filters were then immersed into tubes containing N,N-dimethylformamide (DMF)- and stored in the dark
10 at 4 °C until analyses on shore. Chlorophyll *a* was analysed using a Turner Designs fluorometer pre-calibrated with pure Chl *a* pigment (Suzuki and Ishimaru, 1990).

Samples for heterotrophic prokaryotes were collected from the Niskin bottles and pre-filtered onto disposable 100 μm porosity nylon filters to prevent clogging of any in the flow cytometer. Seawater aliquots of 1.8 cm³ were fixed with 2% (w/v final dilution) formaldehyde solution, quickly frozen in liquid nitrogen and stored in the deep freeze onboard (-60 °C) until analysis at the flow cytometry core facility PRECYM of the Mediterranean Institute of Oceanology (<http://precym.mio.osupytheas.fr>). In the PRECYM, samples were thawed at room temperature and stained using SYBR Green II (Molecular Probes[®]) methods detailed in Marie et al. (1999), Lebaron et al. (1998) and modified by Grégori et al. (2003b). The analyses were performed
20 on a FACSCalibur flow cytometer (BD Biosciences[®]) equipped with an air-cooled argon laser (488 nm, 15 mW). For each particle (cell), five optical parameters were recorded: two light scatter signals, namely forward and right angle light scatters and three fluorescences corresponding to emissions in green (515–545 nm), orange (564–606 nm) and red (653–669 nm) wavelength ranges. Data were collected using the CellQuest software (BD Biosciences[®]) and the analysis and optical resolution of the various groups of heterotrophic prokaryotes were performed a posteriori using

BGD

11, 15793–15826, 2014

Heterotrophic prokaryote distribution in the NPSG

M. Girault et al.

Title Page

Abstract

Introduction

Conclusions

References

Tables

Figures

◀

▶

◀

▶

Back

Close

Full Screen / Esc

Printer-friendly Version

Interactive Discussion



variable groups, namely: the depth-related parameters (phosphate, nitrate, depth), spatial-related parameters (temperature and salinity) and the phytoplankton-related parameters (Chl *a* and silicic acid). This decision was made considering the results of the PCA (environmental variables were separated into three groups).

3 Results

3.1 Sampling sites

The cruise took place along a north–south transect in the western part of the NPSG (141.5° E) during a strong La-Niña climatic event. By using the temperature–salinity diagram, three main areas corresponding to the Kuroshio region (Sta. 1–4), the subtropical gyre (Sta. 5–8) and the Transition zone (Sta. 9–12) were discriminated (Fig. 1) (Girault et al., 2013b). The cruise crossed two main eddies identified in this study as a cold core cyclonic eddy (C), and a warm core anticyclonic eddy (A) (Fig. 1). Eddy C (31° N, 141° E) is located in the Kuroshio region and eddy A (20.5° N, 142° E) in the Transition zone.

3.2 Distribution of the heterotrophic prokaryotes

After staining with the SYBR green II fluorescent dye, three clusters of heterotrophic prokaryotes were identified by different green fluorescence mean intensities: a group of cells with a lower green fluorescence corresponding to heterotrophic prokaryotes with a lower nucleic acid content (LNA), a group of cells displaying a higher green fluorescence corresponding to a higher nucleic acid content (HNA) and a last group of cells with the highest green fluorescence intensity corresponding to the highest nucleic acid content (VHNA) (Fig. 2). Figure 3 shows the abundance of each heterotrophic prokaryote cluster at the surface with latitude. In the surface samples of the Kuroshio region the average concentrations of LNA, HNA and VHNA were 8.71×10^5 , 3.27×10^5 and 2.64×10^5 cells cm⁻³, respectively. In the Subtropical area

Heterotrophic prokaryote distribution in the NPSG

M. Girault et al.

Title Page

Abstract

Introduction

Conclusions

References

Tables

Figures



Back

Close

Full Screen / Esc

Printer-friendly Version

Interactive Discussion



Heterotrophic prokaryote distribution in the NPSG

M. Girault et al.

Title Page

Abstract

Introduction

Conclusions

References

Tables

Figures

◀

▶

◀

▶

Back

Close

Full Screen / Esc

Printer-friendly Version

Interactive Discussion

the average concentrations of LNA, HNA and VHNA were 6.01×10^5 , 2.97×10^5 and 1.84×10^5 cells cm^{-3} , respectively. In the Transition zone the average concentrations of LNA, HNA and VHNA were 5.18×10^5 , 4.38×10^5 and 1.15×10^5 cells cm^{-3} , respectively. Despite the high variability between the concentrations along the north–south transect, the distribution of the three heterotrophic prokaryote groups was characterized by a common maximum at station 4 and a minimum at station 9. At station 4 the concentrations of the LNA, HNA and VHNA were 1.39×10^6 , 5.03×10^5 and 4.35×10^5 cells cm^{-3} , respectively. In contrast, the concentrations of LNA, HNA and VHNA at station 9 were 2.07×10^5 , 1.6×10^5 and 5.07×10^4 cells cm^{-3} , respectively. To a lesser extent, high concentrations of LNA (9.13×10^5 cells cm^{-3}) and HNA (3.62×10^5 cells cm^{-3}) were identified at the northernmost station of the Kuroshio region (at station 1).

The vertical distributions for the concentration of heterotrophic prokaryotes were also investigated along the transect (Fig. 4). As at the surface, the vertical distributions are characterized by lower cell concentrations for all heterotrophic prokaryote groups at station 9. In this station both the LNA and HNA concentrations are significantly lower than at the other stations (Kruskal wallis test, $n = 90$, P value < 0.05). The LNA cluster is numerically dominant in 99% of the flow cytometer samples. The VHNA concentrations are lower than the HNA in 75% of the flow cytometer samples.

Figure 5 displays the ratios of HNA/LNA concentration depending on depth. In the Kuroshio region, ratios are low and varied from 0.29 (Sta. 2) to 0.44 (Sta. 3). In the Subtropical gyre area, the ratios varied from 0.16 (Sta. 5, 70 m) to 0.82 (Sta. 7, 10 m). The higher ratios (up to 1.03 at Sta. 10, 10 m) were observed in the surface layer of the Transition zone. In the Transition zone and the Subtropical gyre area the higher ratios measured were found between the surface and 100 m.

3.3 Statistical analysis

Results of the Principal Component Analysis (PCA) and the Redundance Analysis (RDA) are shown in Figs. 6 and 7, respectively. The correlation circle of the PCA, displays the first two principal components (PC1 and PC2) which accounted for 32.44 and 27.67% of the total inertia, respectively. The third and fourth principal components are not shown due to the low inertia exhibited (11 and 8% of the total inertia, respectively) and the lack of any clear ecological understanding. Silicic acid, Chl *a*, VHNA and LNA were differentiated from temperature and salinity by PC1, while PC2 mainly differentiated depth, nitrate, and phosphate (negative coordinates) from the HNA clusters (positive coordinate). Using hierarchical classification the sampling depths were separated into six different clusters (Table 1 and Fig. 6.) Cluster 1, black dot, characterized all the stations located in the Kuroshio region. Cluster 2 samples were collected at the edge of the Subtropical gyre but also contained the deepest sample collected at station 9 (200m), which was in the anticyclone eddy in the transition zone. All samples in Cluster 3 were collected below a depth of 125m where nitrate and phosphate concentrations were higher than for surface samples. This cluster was defined as the deep layer group. Cluster 4 samples were collected in the center of the subtropical gyre (stations 7 and 8) where heterotrophic prokaryote concentrations were at their maximum in the seawater column. Cluster 5 represented the samples collected in the anticyclonic eddy where a marked salinity has been reported (Girault et al., 2013b). Located in the Transition zone, at the southernmost stations the sixth and last cluster group was characterized by the highest salinity and temperature values. This last cluster (blue dots in the Fig. 6a) is distinguished from the deep layer group (Cluster 3, green dots) by the low nutrient concentrations measured in the upper layer.

A redundancy analysis (Fig. 7) was then performed to find out how the measured environmental factors influenced the distribution of heterotrophic prokaryote subgroups sampled during the cruise. The cumulative percentage of all canonical eigenvalues

BGD

11, 15793–15826, 2014

Heterotrophic prokaryote distribution in the NPSG

M. Girault et al.

Title Page

Abstract

Introduction

Conclusions

References

Tables

Figures

◀

▶

◀

▶

Back

Close

Full Screen / Esc

Printer-friendly Version

Interactive Discussion



Heterotrophic prokaryote distribution in the NPSG

M. Girault et al.

Title Page

Abstract

Introduction

Conclusions

References

Tables

Figures



Back

Close

Full Screen / Esc

Printer-friendly Version

Interactive Discussion



indicated that 69.1 % of the observed heterotrophic cluster variations were explained by environmental factors. The first two axes of the RDA explained 38 and 24 % of the total variance, respectively. Monte-Carlo tests for these two axes were significant (P value < 0.05, using 999 permutations) and suggested that environmental parameters might be important in explaining heterotrophic prokaryote distribution. The first axis is negatively correlated with salinity and positively correlated with the LNA cluster. The second axis is negatively correlated with temperature and the HNA cluster and positively correlated with the VHNA cluster. RDA suggested two main correlations between the LNA cluster and the phytoplankton-related variables (Chl *a* and silicic acid) and the HNA cluster with the depth-related variables (nutrients such as nitrate and phosphate and depth).

To confirm and quantify these possible correlations 4 partial RDAs were also performed: one partial RDA using all the heterotrophic prokaryotes at once and one additional partial RDA for each heterotrophic prokaryote subgroup (LNA, HNA and VHNA). Results of the partial RDA performed on all the heterotrophic prokaryotes showed that among the six environmental variables measured during the cruise, salinity and temperature statistically contribute for 24 and 7.5 % of the variation of the heterotrophic prokaryotes, respectively. To a lesser extent, phosphate alone explained 3.5 % of the variability, whereas Chl *a*, nitrate, depth and silicic acid explained only 1.8, 1.7, 1.7 and 0.86 %, respectively. The partial RDAs performed either on LNA, or HNA, or VHNA indicated that environmental parameters can explain 60, 55 and 27 % of the total variance, respectively (Table 2). Partial RDA results showed that the spatial-related parameters alone can explain up to 31 % of the variation in the heterotrophic prokaryote distribution. The depth-related parameters explained between 6 and 8 % of the variance and finally the phytoplankton-related group explained a maximum 4 % of the variance in the LNA heterotrophic prokaryotes. As far as the HNA cluster is concerned, the joint variation of the spatial- and phytoplankton-related parameters explained 22 % of the variance.

4 Discussion

4.1 Relationship between the heterotrophic prokaryotes and phytoplankton along the oligotrophic gradient

The spatial distribution of the heterotrophic prokaryote clusters defined by flow cytometry can be discriminated into three main areas that correspond to different seawater masses: (i) the Kuroshio region, where the highest heterotrophic prokaryote concentrations were measured, (ii) the Subtropical gyre and (iii) the Transition zone both characterized by a high variability in the heterotrophic prokaryote concentrations in the seawater column (Figs. 1, 3 and 4). Separation between the Subtropical gyre and the Transition zone was made using the salinity front observed south of station 8 (Girault et al., 2013b). The hierarchical classification performed on the first two axes of the PCA, statistically confirmed this latitudinal pattern and also provided additional information on the relationships between the environmental parameters and specific mesoscale structures encountered during the cruise. Discrimination of six different clusters highlighted the complex assemblages of the mesoscale structures in the three main areas as previously reported in the NPSG area (Aoki et al., 2002) (Fig. 6). For example, stations located in the Transition zone were statistically discriminated into two clusters (Clusters 5 and 6) due to the high salinity and temperature values in the anticyclonic eddy (station 9). In addition to the latitudinal variations, vertical distribution is also important and this is taken into consideration with cluster 3. This cluster grouped the deep layer samples which were characterized by higher nutrient concentrations than found in the upper layer (negative coordinates on PCA2). An interesting result obtained from the PCA and RDA, is that PC1 characterized both the silicic acid and Chl *a* concentrations. Although low concentrations of silicic acid have been reported in cyclonic mesoscale eddies, the effect of silicic acid on phytoplankton over a larger scale is unexpected, as the lowest concentrations of phosphate and nitrate have been reported in the euphotic layer of the western part of the NPSG area (Hashihama et al., 2009, 2014). The Si : N : P stoichiometry measured during the Tokyo–Palau cruise

Heterotrophic prokaryote distribution in the NPSG

M. Girault et al.

Title Page

Abstract

Introduction

Conclusions

References

Tables

Figures



Back

Close

Full Screen / Esc

Printer-friendly Version

Interactive Discussion



mechanism initiated by the concentration of VHNA may partially lead to the high abundance of LNA observed at the bottom of the euphotic layer (Thyssen et al., 2005).

5 Conclusions

This study along a 2300 km transect in the North Pacific subtropical gyre area during a strong La Niña condition showed that the heterotrophic prokaryote distribution is correlated with three different seawater masses identified as (i) the Kuroshio, (ii) the Subtropical gyre and (iii) the Transition zone. A latitudinal increase in the HNA/LNA ratio was found along the oligotrophic gradient and suggested different relationships between the various heterotrophic clusters and the environmental variables measured in situ during the cruise. The statistical analyses highlighted that the majority of the heterotrophic prokaryote distribution is explained by temperature and salinity. Nutrients and phytoplankton-related variables had different influences depending on the LNA, HNA and VHNA clusters. LNA distribution is mainly correlated with temperature and salinity while HNA distribution is mainly explained by an association of variables (temperature, salinity, Chl *a* and silicic acid). During the cruise, two eddies (one cyclonic and one anticyclonic) were crossed. The vertical distributions of LNA, HNA and VHNA were investigated. Based on the current surface map and the microorganism distribution, it is reasonable to form the hypothesis that the high concentration of heterotrophic prokaryotes observed at station 4 was linked to the path of the cold cyclonic eddy core. In contrast, in the warm core of the anticyclonic eddy, lower heterotrophic prokaryote concentrations are suggested to be linked to the low nutrient concentrations. All the results described in this study highlight the high variability of each heterotrophic prokaryote cluster defined by their nucleic acid content (LNA, HNA, and VHNA) with regard to the mesoscale structures and the oligotrophic gradient observed in situ within the area of the North Pacific subtropical gyre.

Acknowledgements. We thank Captain Akira Noda, crew members of the RT/V *Shinyo maru* of Tokyo University of Marine Science and Technology, (TUMSAT) for their cooperation at sea.

Heterotrophic prokaryote distribution in the NPSG

M. Girault et al.

Title Page

Abstract

Introduction

Conclusions

References

Tables

Figures



Back

Close

Full Screen / Esc

Printer-friendly Version

Interactive Discussion



We appreciated the English correction of the manuscript made by Tracy L. Bentley. We thank Yuta Nakagawa and Shinko Kinouchi for their help during the cruise. We are grateful to the Mediterranean Institute of Ocenaography (MIO) for the flow cytometry analyses. We also thank the Soci  t   franco-japonaise d'Oc  anographie for its support in shipping the samples from Japan to France.

References

- Andrade, L., Gonzalez, A. M., Rezende, C. E., Suzuki, M., Valentin, J. L., and Paranhos, R.: Distribution of HNA and LNA bacterial groups in the Southwest Atlantic Ocean, *Braz. J. Microbiol.*, 38, 330–336, 2007.
- Aoki, Y., Suga, T., and Hanawa, K.: Subsurface subtropical fronts of the North Pacific as inherent boundaries in the ventilated thermocline, *J. Phys. Oceanogr.*, 32, 2299–2311, 2002.
- Ar  stegui, J. and Montero, M. F.: Temporal and spatial changes in plankton respiration and biomass in the Canary Islands region: the effect of mesoscale variability, *J. Marine Syst.*, 54, 65–82, 2005.
- Baines, S. B., Twining, B. S., Brzezinski, M. A., and Nelson, D. M.: An unexpected role for picocyanobacteria in the marine silicon cycle, *Nat. Geosci.*, 5, 886–891, 2012.
- Baltar, F., Ar  stegui, J., Montero, M. F., Espino, M., Gasol, J. M., and Herndl, G. J.: Mesoscale variability modulates seasonal changes in the trophic structure of nano- and picoplankton communities across the NW Africa–Canary Islands transition zone, *Prog. Oceanogr.*, 83, 180–188, 2009.
- Baltar, F., Ar  stegui, J., Gasol, J. M., Lekunberri, I., and Herndl, G. J.: Mesoscale eddies: 10 hotspots of prokaryotic activity and differential community structure in the ocean, *ISME J.*, 4, 975–988, 2010.
- Bidigare, R. R., Benitez-Nelson, C., Leonard, C. L., Quay, P. D., Parsons, M. L., Foley, D. G., and Seki, M. P.: Influence of a cyclonic eddy on microheterotroph biomass and carbon export in the Lee of Hawaii, *Geophys. Res. Lett.*, 30, 51, 1–4, 2003.
- Bidle, K. D. and Azam, F.: Accelerated dissolution of diatom silica by marine bacterial assemblages, *Nature*, 397, 508–512, 1999.

Heterotrophic prokaryote distribution in the NPSG

M. Girault et al.

Title Page

Abstract

Introduction

Conclusions

References

Tables

Figures

◀

▶

◀

▶

Back

Close

Full Screen / Esc

Printer-friendly Version

Interactive Discussion



Heterotrophic prokaryote distribution in the NPSG

M. Girault et al.

Title Page

Abstract

Introduction

Conclusions

References

Tables

Figures

◀

▶

◀

▶

Back

Close

Full Screen / Esc

Printer-friendly Version

Interactive Discussion



Bouvier, T., del Giorgio, P. A., and Gasol, J. M.: A comparative study of the cytometric characteristics of high and low nucleic-acid bacterioplankton cells from different aquatic ecosystems, *Environ. Microbiol.*, 9, 2050–2066, 2007.

Brown, S. L., Landry, M. R., Neveux, J., and Dupouy, C.: Microbial community abundance and biomass along a 180° transect in the equatorial Pacific during an El Niño-Southern Oscillation cold phase, *J. Geophys. Res.*, 108, 8139, doi:10.1029/2001JC000817, 2003.

Campbell, L., Liu, H., Nolla, H. A., and Vaulot, D.: Annual variability of phytoplankton and bacteria in the subtropical North Pacific Ocean at station ALOHA during the 1991–1994 ENSO event, *Deep-Sea Res. Pt. I*, 44, 167–192, 1997.

Currie, D. J. and Kalf, J.: Can bacteria outcompete phytoplankton for phosphorus? A chemostat test, *Microb. Ecol.*, 10, 205–216, 1984.

Duhamel, S., Dyrhman, S. T., and Karl, D. M.: Alkaline phosphatase activity and regulation in the North Pacific Subtropical Gyre, *Limnol. Oceanogr.*, 55, 1414–1425, 2010.

Garside, C.: A chemiluminescent technique for the determination of nanomolar concentrations of nitrate and nitrite in seawater, *Mar. Chem.*, 11, 159–167, 1982.

Gasol, J. M., Zweifel, U. L., Peters, F., Fuhrman, J. A., and Hågström, A.: Significance of size and nucleic acid content heterogeneity as measured by flow cytometry in natural planktonic bacteria, *Appl. Environ. Microb.*, 65, 4475–4483, 1999.

Girault, M., Arakawa, H., and Hashihama, F.: Phosphorus stress of microphytoplankton community in the western subtropical North Pacific, *J. Plankton Res.*, 35, 146–157, 2013a.

Girault, M., Arakawa, H., Barani, A., Ceccaldi, H. J., Hashihama, F., Kinouchi, S., and Gregori, G.: Distribution of ultraphytoplankton in the western part of the North Pacific subtropical gyre during a strong La Niña condition: relationship with the hydrological conditions, *Biogeosciences*, 10, 5947–5965, doi:10.5194/bg-10-5947-2013, 2013b.

Grégori G., Citterio, S., Ghiani, A., Labra, M., Sgorbati, S., Brown, S., and Denis, M.: Resolution of viable and membrane compromised bacteria in fresh and marine waters based on analytical flow cytometry and nucleic acid double staining, *Appl. Environ. Microb.*, 67, 4662–4670, 2001.

Grégori, G., Denis, M., Lefevre, D., and Romano, J. C.: Viability of heterotrophic bacteria in the Bay of Marseilles, *C. R. Biol.*, 326, 739–750, 2003a.

Grégori, G., Denis, M., Sgorbati, S., and Citterio, S.: Resolution of viable and membrane-compromised free bacteria in aquatic environments by flow cytometry, *Curr. Protoc. Cytom.*, 23, 11.15.1–11.15.7, 2003b.

Heterotrophic prokaryote distribution in the NPSG

M. Girault et al.

Title Page

Abstract

Introduction

Conclusions

References

Tables

Figures

◀

▶

◀

▶

Back

Close

Full Screen / Esc

Printer-friendly Version

Interactive Discussion



Hall, E. K., Neuhauser, C., and Cotner, J.: toward a mechanistic understanding of how natural bacterial communities respond to changes in teperature in aquatic ecosystems, *ISME J.*, 2, 471–481, 2008.

Hashihama, F. and Kanda, J.: Automated colorimetric determination of trace silicic acid in seawater by gas-segmented continuous flow analysis with a liquid waveguide capillary cell, *La Mer*, 47, 119–127, 2010.

Hashihama, F., Furuya, K., Kitajima, S., Takeda, S., Takemura, T., and Kanda, J.: Macro-scale exhaustion of surface phosphate by dinitrogen fixation in the western North Pacific, *Geophys. Res. Lett.*, 36, L03610, doi:10.1029/2008GL036866, 2009.

Hashihama, F., Kanda, J., Maeda, Y., Ogawa, H., and Furuya, K.: Selective depressions of surface silicic acid within cyclonic mesoscale eddies in the oligotrophic western North Pacific, *Deep-Sea Res. Pt. I*, 90, 115–124, 2014.

Kataoka, T., Hodoki, Y., Suzuki, K., Saito, H., Higashi, S.: Tempo-spatial patterns of bacterial community composition in the western North Pacific Ocean, *J. Marine Syst.*, 77, 197–207, 2009.

Klein, P. and Lapeyre, G.: The oceanic vertical pump induced by mesoscale and submesoscale turbulence, *Annual Review of Marine Science*, 1, 351–375, 2009.

Kobari, T., Hijjiya, K., Minowa, M., and Kitamura, M.: Depth distribution, biomass and taxonomic composition of subtropical microbial community in southwestern Japan, *South Pacific Studies*, 32, 31–43, 2011.

Krause, J. W., Brzezinski, M. A., Villareal, T. A., and Wilson, C.: Increased kinetic efficiency for silicic acid uptake as a driver of summer diatom blooms in the North Pacific subtropical gyre, *Limnol. Oceanogr.*, 57, 1084–1098, 2012.

Landry, M. R., Brown, S. L., Rii, Y. M., Selph, K. E., Bidigare, R. R., Yang, E. J., and Simmons, M. P.: Depth-stratified phytoplankton dynamics in Cyclone Opal, a subtropical mesoscale eddy, *Deep-Sea Res. Pt. II*, 56, 1348–1359, 2008.

Lasternas, S., Piedeleu, M., Sangrà, P., Duarte, C. M., and Agustí, S.: Forcing of dissolved organic carbon release by phytoplankton by anticyclonic mesoscale eddies in the subtropical NE Atlantic Ocean, *Biogeosciences*, 10, 2129–2143, doi:10.5194/bg-10-2129-2013, 2013.

Lebaron, P., Parthuisot, N., and Catala, P.: Comparison of blue nucleic acid dyes for flow cytometric enumeration of bacteria in aquatic systems, *Appl. Environ. Microb.*, 64, 1725–1730, 1998.

Heterotrophic prokaryote distribution in the NPSG

M. Girault et al.

Title Page

Abstract

Introduction

Conclusions

References

Tables

Figures

◀

▶

◀

▶

Back

Close

Full Screen / Esc

Printer-friendly Version

Interactive Discussion



- Stapleton, N. R., Aicken, W. T., Dovey, P. R., and Scott, J. C.: The use of radar altimeter data in combination with other satellitesensors for routine monitoring of the ocean: case study of the northern Arabian sea and Gulf of Guam, *Can. J. Remote Sens.*, 28, 567–572, 2002.
- Suzuki, R. and Ishimaru, T.: An improved method for the determination of phytoplankton chlorophyll using N,N-Dimethylformamide, *J. Oceanogr. Soc. Jpn.*, 46, 190–194, 1990.
- Sweeney, E. N., McGillicuddy, D. J., and Buesseler, K. O.: Bio-geochemical impacts due to mesoscale eddy activity in the sargasso sea as measured at the bermuda atlantic time-series study (BATS), *Deep-Sea Res. Pt. II*, 50, 3017–3039, 2003.
- Thingstad, T. F., Zweifel, U. L., and Assoulezadegan, F. R.: P-limitation of heterotrophic bacteria and phytoplankton in the north-west Mediterranean, *Limnol. Oceanogr.*, 43, 88–94, 1998.
- Thomson, R. E. and Fine, I. V.: Estimating mixed layer depth from oceanic profile data, *J. Atmos. Ocean. Tech.*, 20, 319–329, 2003.
- Thyssen, M., Lefèvre, D., Caniaux, G., Ras, J., Fernández, C. F., and Denis, M.: Spatial distribution of heterotrophic bacteria in the northeast Atlantic (POMME study area) during spring 2001, *J. Geophys. Res.*, 110, C07S16, doi:10.1029/2004JC002670, 2005.
- Vadstein, O.: Evaluation of competitive ability of two heterotrophic planktonic bacteria under phosphorus limitation, *Aquat. Microb. Ecol.*, 14, 119–127, 1998.
- Vaillancourt, R. D., Marra, J., Seki, M. P., Parsons, M. L., and Bidigare, R. R.: Impact of a cyclonic eddy on phytoplankton community structure and photosynthetic competency in the subtropical North Pacific Ocean, *Deep-Sea Res. Pt. I*, 50, 829–847, 2003.
- Van Wambeke, F., Catala, P., Pujo-Pay, M., and Lebaron, P.: Vertical and longitudinal gradients in HNA-LNA cell abundances and cytometric characteristics in the Mediterranean Sea, *Biogeosciences*, 8, 1853–1863, doi:10.5194/bg-8-1853-2011, 2011.
- Vernet, M. and Lorenzen, C. J.: The presence of chlorophyll b and the estimation of phaeopigments in marine phytoplankton, *J. Plankton Res.*, 9, 265–265, 1987.
- Wang, H., Smith, H. L., Kuang, Y., and Elser, J. J.: Dynamics of stoichiometric bacteria-algae interactions in the epilimnion, *Siam J. Appl. Math.*, 68, 503–522, 2007.
- Yamada, N., Fukuda, H., Ogawa, H., Saito, H., and Suzumura, M.: Heterotrophic bacterial production and extracellular enzymatic activity in sinking particulate matter in the western North Pacific Ocean, *Front. Microbiol.*, 3, 379, doi:10.3389/fmicb.2012.00379, 2012.
- Zubkov, M. V., Fuchs, B. M., Burkill, P. H., and Amann, R.: Comparison of cellular and biomass specific activities of dominant bacterioplankton groups in stratified waters of the Celtic Sea, *Appl. Environ. Microb.*, 67, 5210–5218, 2001.

Table 1. List of observations from stations 1 to 11 and their classification into six clusters according to the principal component analysis (PCA).

PCA Cluster	Observations	Latitude (° N)	Station	Depth (m)
1	1	33.6	1	0
1	2	33	2	0
1	3	31.6	3	0
1	4	31	4	0
2	5, 6, 7, 8, 9, 10, 11, 12, 13	28.6	5	0, 40, 60, 70, 78, 80, 100, 120, 140
2	15, 16, 17, 18, 19, 20, 21, 22, 23	27.1	6	0, 25, 60, 75, 80, 90, 100, 115, 125
2	32, 33, 34	24.5	7	75, 90, 101
2	40, 41	22.5	8	110, 125
2	55	20.5	9	200
3	14	28.6	5	160
3	24	27.1	6	150
3	42, 43, 44	22.5	8	135, 150, 165
3	54	20.5	9	160
3	61	19.6	10	125
4	25, 26, 27, 28, 29, 30, 31	24.5	7	0, 10, 25, 40, 58, 59, 60
4	35, 36, 37, 38, 39	22.5	8	0, 25, 50, 75, 95
5	45, 46, 47, 48, 49, 50, 51, 52, 53	20.78	9	0, 25, 50, 75, 100, 120, 130, 140
5	59, 60, 62	19.6	10	75, 100, 150
6	56, 57, 58	19.6	10	0, 25, 50
6	63, 64, 65, 66	17.2	11	0, 30, 45, 60

Heterotrophic prokaryote distribution in the NPSG

M. Girault et al.

Title Page

Abstract

Introduction

Conclusions

References

Tables

Figures

◀

▶

◀

▶

Back

Close

Full Screen / Esc

Printer-friendly Version

Interactive Discussion



Heterotrophic prokaryote distribution in the NPSG

M. Girault et al.

[Title Page](#)

[Abstract](#)

[Introduction](#)

[Conclusions](#)

[References](#)

[Tables](#)

[Figures](#)

[◀](#)

[▶](#)

[◀](#)

[▶](#)

[Back](#)

[Close](#)

[Full Screen / Esc](#)

[Printer-friendly Version](#)

[Interactive Discussion](#)



Table 2. Partial redundancy analysis performed on each heterotrophic prokaryote cluster optically resolved by flow cytometry: low nucleic acid content (LNA), high nucleic acid content (HNA) and very high nucleic acid content (VHNA). According to the PCA results, Chl *a* and silicic acid are the phytoplankton-related variables. Temperature and salinity are the spatial-related variables. Nitrate, phosphate and depth are the depth-related variables. Negative values characterized the lack of any correlation between heterotrophic prokaryote clusters and the variables tested.

		LNA	HNA	VHNA
Total explained variance		60 %	55 %	27 %
Joint variation	Phytoplankton-related and spatial- and depth-related	6 %	−1 %	−1 %
Partial joint variation	Spatial-related and phytoplankton-related	−1 %	22 %	−4 %
	Spatial- and depth-related	9 %	1 %	5 %
	Depth-related and phytoplankton-related	3 %	1 %	0 %
Unique variation	Phytoplankton-related	4 %	1 %	1 %
	Depth-related	8 %	8 %	6 %
	Spatial-related	31 %	23 %	20 %

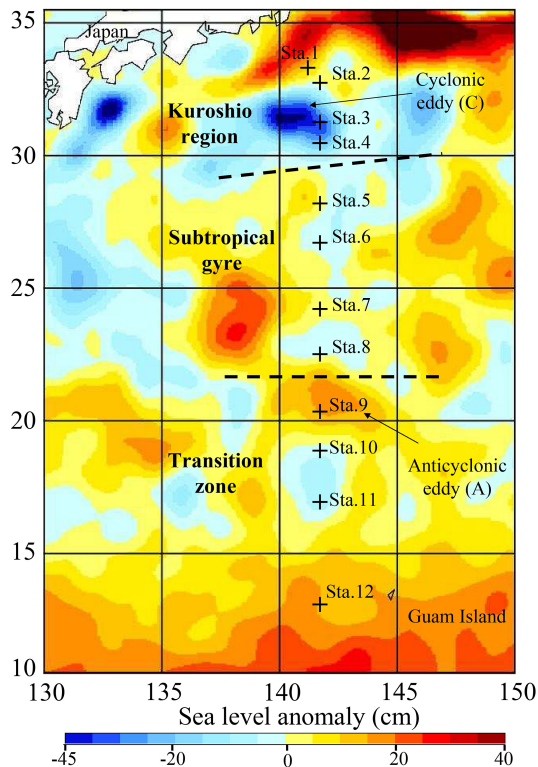


Figure 1. Map of the sea level anomaly (cm) in the west part of the North Pacific subtropical gyre. The sampling stations (black crosses) were separated depending on temperature and salinity into 3 areas: Kuroshio region (stations 1–4), Subtropical gyre (stations 5–8) and the Transition zone (stations 9–12).

Heterotrophic prokaryote distribution in the NPSG

M. Girault et al.

Title Page

Abstract Introduction

Conclusions References

Tables Figures

◀ ▶

◀ ▶

Back Close

Full Screen / Esc

Printer-friendly Version

Interactive Discussion



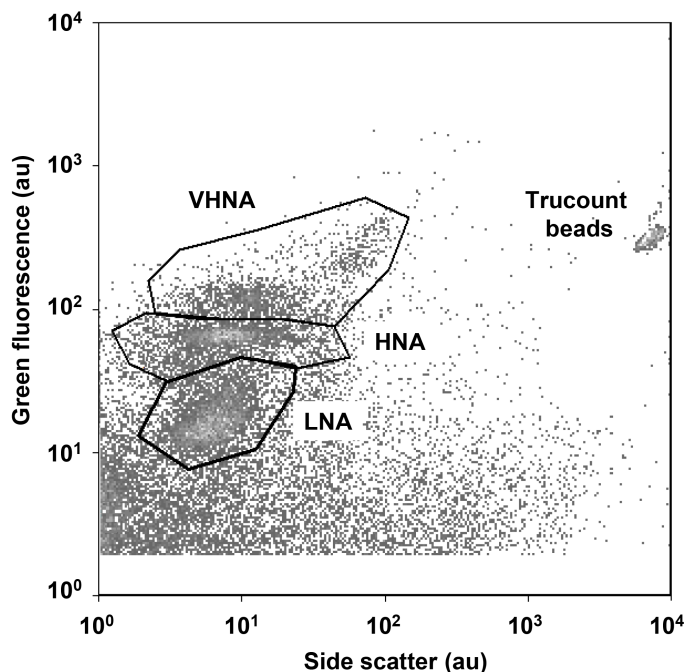


Figure 2. Example of the optical resolution obtained by the analytical flow cytometry of the heterotrophic prokaryote assemblages sampled during the Tokyo–Palau cruise at station 8 (25 m depth). Cytogram of green fluorescence intensity (SYBR Green II[®]) vs. side scatter intensity showed up three groups of heterotrophic prokaryotes: one defined by prokaryotes with a low nucleic acid content (LNA), one defined by prokaryotes with a high nucleic acid content (HNA) and one defined by those with a very high nucleic acid content (VHNA). Trucount calibration beads (Beckton Dickinson[®]) were used both as an internal standard and to determine the volume analysed by the flow cytometer.

Heterotrophic prokaryote distribution in the NPSG

M. Girault et al.

[Title Page](#)

[Abstract](#) | [Introduction](#)

[Conclusions](#) | [References](#)

[Tables](#) | [Figures](#)

[◀](#) | [▶](#)

[◀](#) | [▶](#)

[Back](#) | [Close](#)

[Full Screen / Esc](#)

[Printer-friendly Version](#)

[Interactive Discussion](#)



Heterotrophic prokaryote distribution in the NPSG

M. Girault et al.

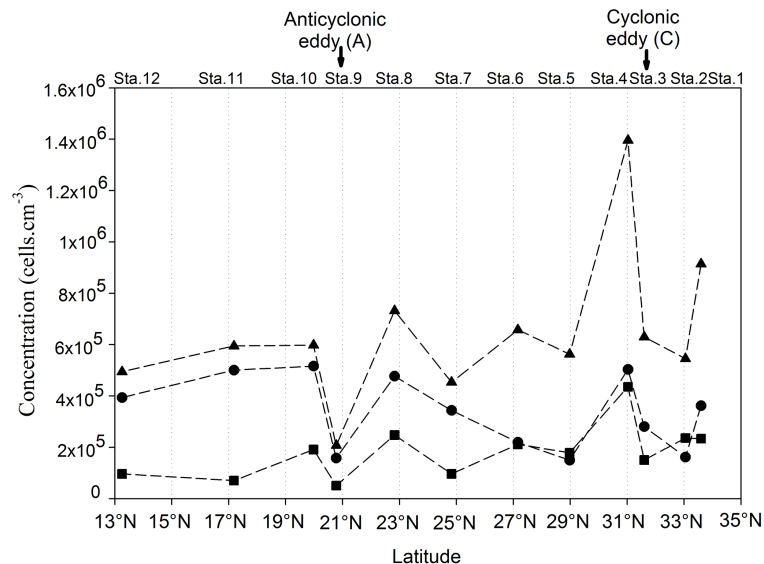


Figure 3. Latitudinal distribution of the heterotrophic prokaryote abundances at the surface along the 141.5° E meridian. (▲) is LNA heterotrophic prokaryotes, (●) the HNA heterotrophic prokaryotes and (■) the VHNA heterotrophic prokaryotes. Sampling stations are indicated on the upper scale axis.

Title Page

Abstract

Introduction

Conclusions

References

Tables

Figures

◀

▶

◀

▶

Back

Close

Full Screen / Esc

Printer-friendly Version

Interactive Discussion



Heterotrophic prokaryote distribution in the NPSG

M. Girault et al.

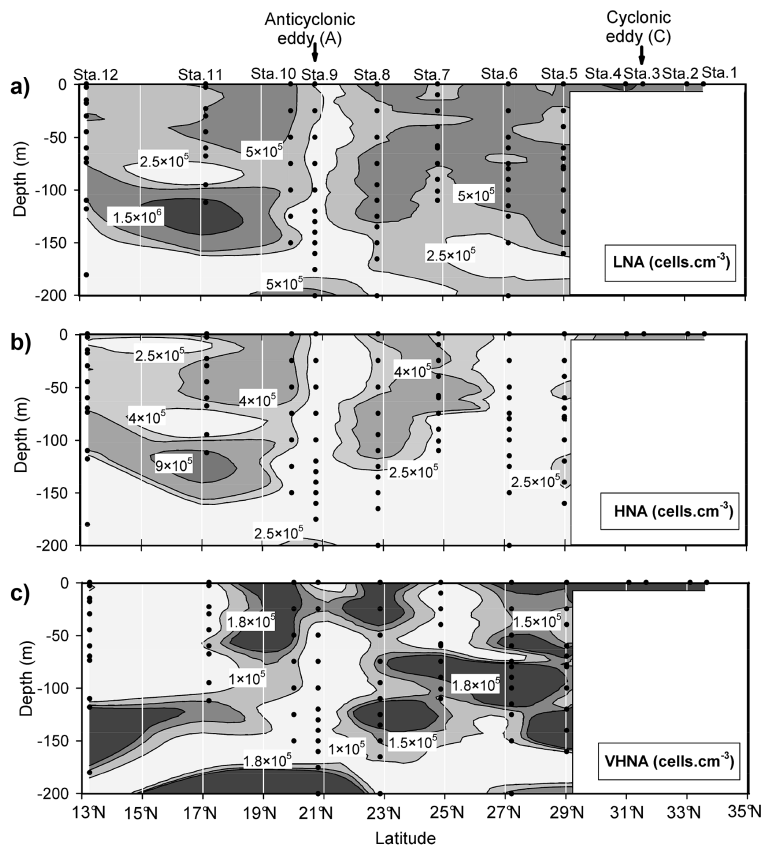


Figure 4. Vertical concentration (cells cm⁻³) of LNA, HNA, and VHNA heterotrophic prokaryotes interpolated along the transect during the Tokyo–Palau Cruise. The black dots are the depths sampled.

Heterotrophic prokaryote distribution in the NPSG

M. Girault et al.

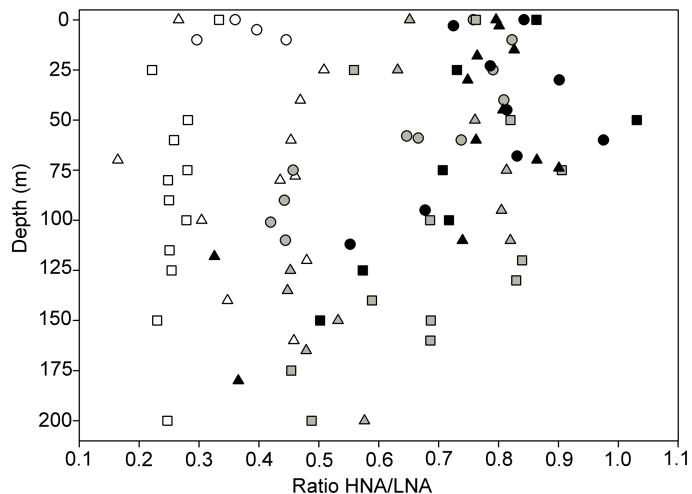


Figure 5. Ratios of the abundance of HNA heterotrophic prokaryotes to the abundance of LNA heterotrophic prokaryotes with depth. The white circles are stations 1, 2, 3 and 4. The white triangles and the squares are stations 5 and 6, respectively. The grey circles, triangles, and squares characterize stations 7, 8, 9, respectively. The black squares, circles and triangles are stations 10, 11 and 12, respectively.

[Title Page](#)[Abstract](#)[Introduction](#)[Conclusions](#)[References](#)[Tables](#)[Figures](#)[◀](#)[▶](#)[◀](#)[▶](#)[Back](#)[Close](#)[Full Screen / Esc](#)[Printer-friendly Version](#)[Interactive Discussion](#)

Heterotrophic prokaryote distribution in the NPSG

M. Girault et al.

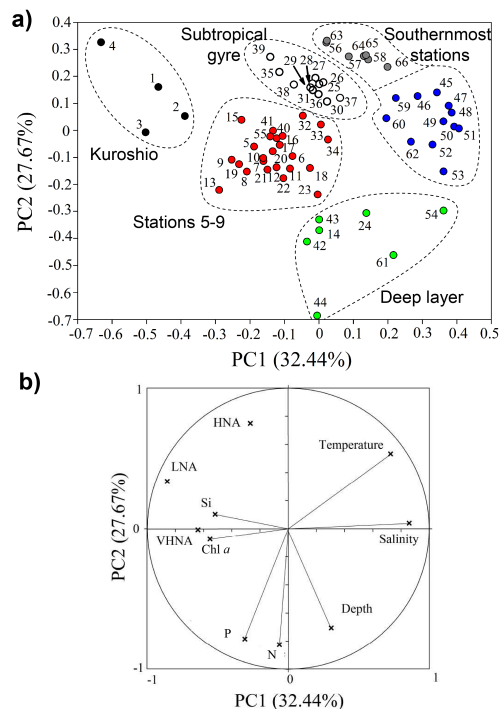


Figure 6. Hierarchical clustering illustrated for the first two principal components of the principal component analysis performed with the data collected from stations 1 to 11 (a). According to the classification (Table 1) the sampling depths (numbers) were discriminated into 6 clusters: one characterizes the Kuroshio region (Cluster 1, black), another incorporates stations 5 to 9 (Cluster 2, red), a third one the deep layer (Cluster 3, green) and the last three clusters characterize the subtropical gyre (Cluster 4, white) and the southernmost stations (5, blue and 6, dark grey). The circle (b) shows the first two dimensions of the principal component analysis. The environmental variables taken into consideration are temperature, salinity, depth, nitrate (N), phosphate (P), silicic acid (Si), and chlorophyll *a* (Chl *a*).

Title Page

Abstract

Introduction

Conclusions

References

Tables

Figures

◀

▶

◀

▶

Back

Close

Full Screen / Esc

Printer-friendly Version

Interactive Discussion



Heterotrophic prokaryote distribution in the NPSG

M. Girault et al.

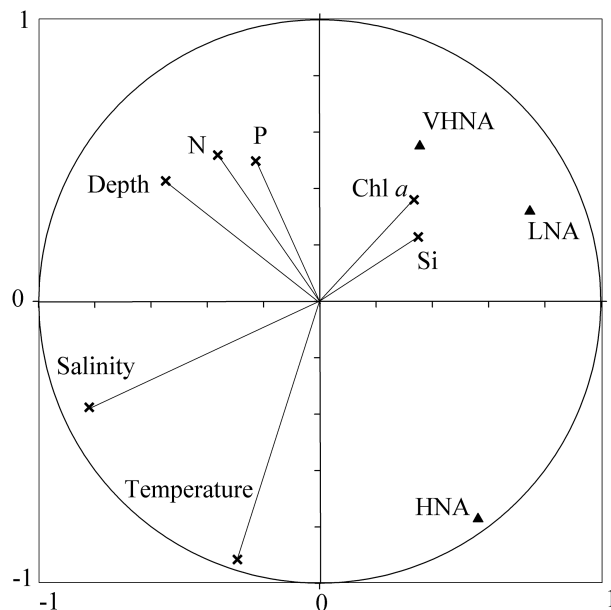


Figure 7. Correlation plot of the redundancy analysis (RDA) on the relationships between the environmental variables and the three subgroups of heterotrophic prokaryotes observed during the cruise (LNA, HNA, VHNA). Chl *a*, N, P, and Si stand for chlorophyll *a*, nitrate, phosphate, and silicic acid, respectively.

[Title Page](#)[Abstract](#)[Introduction](#)[Conclusions](#)[References](#)[Tables](#)[Figures](#)[◀](#)[▶](#)[◀](#)[▶](#)[Back](#)[Close](#)[Full Screen / Esc](#)[Printer-friendly Version](#)[Interactive Discussion](#)